Biomed Microdevices
DOI 10.1007/s10544-012-9671-6

Formation of lipid bilayers inside microfluidic channel array for monitoring membrane-embedded nanopores of phi29 DNA packaging nanomotor

Joon S. Shim · Jia Geng · Chong H. Ahn · Peixuan Guo

Abstract An efficient method to form lipid bilayers inside an array of microfluidic channels has been developed and applied to monitor the membrane-embedded phi29 DNA packaging motor with an electrochemical characterization on a lab-on-a-chip (LOC) platform. A push-pull junction capturing approach was applied to confine a small amount of the lipid solution inside a microchannel. The selective permeability between solvents and water in PDMS was utilized to extract the solvent from the lipid solution, resulting in a self-formation of the lipid bilayer in the microchannel array. Each microchannel was independently connected to a silver/silver chloride (Ag/AgCl) electrode array, leading to a high-throughput monitoring of the nanopore insertion in the formed lipid bilayers. The formation of multiple lipid bilayers inside an array of microchannels and the simultaneous electrical and optical monitoring of multiple bilayer provides an efficient LOC platform for the further development of single phi29 motor pore sensing and high throughput single pore dsDNA sequencing.

Keywords Lipid bilayer · Push-pull junction capturing · Nano Channel · Single Pore Conductance · High throughput DNA sequencing · Viral DNA packaging Motor

Electronic supplementary material The online version of this article (doi:10.1007/s10544-012-9671-6) contains supplementary material, which is available to authorized users.

J. S. Shim · J. Geng · C. H. Ahn (✉) · P. Guo (✉)
College of Engineering and Applied Science,
University of Cincinnati,
Cincinnati, OH 45221, USA
e-mail: chong.ahn@uc.edu
e-mail: peixuan.guo@uky.edu

Published online: 07 July 2012

1 Introduction

Artificial lipid bilayers have been intensively investigated due to their structural similarity to cellular membranes. Suspended lipid bilayers are usually formed by painting a lipid solution at a small hole through a thin polymer film. However, forming an array of multiple lipid bilayers in this manner requires a lot of labor. Additionally, in order to characterize the formed lipid bilayer, a pair of silver/silver chloride (Ag/AgCl) electrodes should be inserted in either side of the lipid bilayer. For the multiple measurements, this repeated insertion of Ag/AgCl electrodes easily contaminates the sample solutions, and thus requires the intense manual labor of cleaning the electrodes before each insertion. Furthermore, the thin lipid bilayer could be easily broken down during inserting the electrodes. Thus, a Lab-on-a-Chip (LOC) platform with patterned electrodes inside each microchannel is very desirable for highly precise and automatic on-chip analysis of nanopore biosensors (Oosterbroek and Berg van den 2003; Manz et al. 1998; Yager et al. 2006; Ahn et al. 2004).

Various trials have been executed to form the lipid bilayer in a LOC platform (Suzuki and Takeuchi 2008; Sandison et al. 2007; Suzuki et al. 2006; Funakoshi et al. 2006; Suzuki et al. 2007). In order to mimic insertion of channel proteins in a cellular membrane, lipid membrane should have a bilayer quality (Suzuki and Takeuchi 2008). For this purpose, the lipid bilayer was exposed to air for solvent drainage between the lipid film (Sandison et al. 2007), and pressure was applied to thin the lipid membrane (Sandison et al. 2007; Suzuki et al. 2006; Funakoshi et al. 2006). Also, the solvent permeable property of PDMS was adopted to absorb the solvent from the lipid solution (Malmstadt et al. 2006). Utilizing these techniques to thin the lipid membrane up to the bilayer quality, multiple arrays of lipid bilayers was

formed in a microfabricated parylene membrane (Osaki et al. 2009; Le Pioufle et al. 2008). The array of microchamber was utilized to make the thin lipid bilayer inside the microchannel (Ota et al. 2011). Recently, the formation of the lipid bilayer in 96 well plate was achieved by injecting a droplet to the interface between the lipid-containing oil and the water (Poulos et al. 2009).

In spite of these advances to achieve the parallelized formation of lipid bilayers, there are still large demands to implement the lipid bilayer array on the automated LOC platform. Because the lipid bilayers are usually fragile and maintained for a short time, the lipid bilayer should be automatically generated with a simple and rapid process. Also, the electrodes need to be independently connected to each lipid bilayer to avoid the laborious steps of cleaning and insertion of the electrodes for multiple measurements. Finally, the multiple arrays of lipid bilayer should be reliably formed in a microchannel with a high yield of success.

Biological systems contain a wide variety of nanomachines and highly-ordered structures with diverse functions. Bacteriophage phi29 packages its genome into a preformed procapsid shell with the aid of a nanomotor (Guo et al. 1987a, b). This motor (Guo 2002; Aathavan et al. 2009) is comprised of a protein core called connector, six copies of pRNA (packaging RNA) (Zhang et al. 1998; Guo et al. 1987a; Guo et al. 1998; Shu et al. 2007), and DNA packaging protein gp16. The connector consists of 12 copies of protein gp10, which encircle to form a dodecameric channel with 3.6 nm at its narrowest part. The channel acts as a path for the translocation of dsDNA and has inspired its application in nanotechnology. Recently, we inserted the phi29 motor channel into the lipid bilayer (Wendell et al. 2009; Jing et al. 2010a, b; Geng et al. 2011; Fang et al. 2012; Haque et al. 2012). The membrane embedded connector has been shown to exhibit robust properties and generate extremely reliable, precise and sensitive conductance signatures in single channel conductance measurements (Wendell et al. 2009; Jing et al. 2010a). The conductance of each pore was almost identical and perfectly linear with respect to the applied voltage. The connector channel has been shown to be stable under a wide range of experimental conditions, including high salt and extreme pH level (Jing et al. 2010a, b; Fang et al. 2012). The connector channel displays one-way traffic property for DNA trafficking from N-terminal entrance to C-terminal exit (Jing et al. 2010b). Additionally, the robust connector has a larger channel allowing for the passage of both dsDNA and ssDNA with a one way-traffic property (Jing et al. 2010b). Large scale production of the connector has already been achieved (Wendell et al. 2009; Ibanez et al. 1984; Robinson et al. 2006; Guo et al. 2005; Xiao et al. 2009; Cai et al. 2008). These features make the phi29 connector an ideal candidate for single molecule sensing (Haque et al. 2012) and high throughput single pore genomic DNA sequencing. The larger pore size is also advantageous to functionalize the pore by inserting or conjugating chemical groups to selectively detect a target DNA or to control the speed of translocation. For a practical implementation of the nanopore biosensor, an on-chip monitoring of pore protein embedded membrane should be implemented on a LOC platform.

In this report, a LOC device was implemented for high throughput screening. By capturing a small amount of the lipid solvent at the junction of microchannel, multiple lipid bilayers inside the array were reliably created within the microchannel. Also, each microchannel was independently connected to an Ag/AgCl electrode array, allowing a simultaneous recording of multiple lipid bilayers during the translocation of DNAs through the nanopore in real time. Furthermore, the pore protein of phi29 was successfully inserted into the formed lipid bilayers with an electrical monitoring of the interactions. As a result, the multiple formations of nanopore-embedded lipid bilayers inside a microchannel provides an efficient LOC platform for further development of single pore sensing and high throughout single pore dsDNA sequencing.

2 Principle

The basic principle of lipid bilayer formation inside microchannels utilizes the porous material property of PDMS where air and solutions are permeable (Malmstadt et al. 2006; McDonald and Whitesides 2002). This permeable property of PDMS enables the selective extraction of the solvent from a lipid solution. After this selective extraction of the solvent, a membrane of lipids bilayer is self-assembled due to a molecular property of the individual lipid. Each lipid molecule consists of a hydrophilic head and a hydrophobic tail, where the hydrophilic head of the lipid tends to contact water, while the tail of lipid contacts hydrophobic solvent. When a small volume of the solvent with dispersed lipids is captured inside a microchannel, the dispersed lipids in the solvent assemble the lipid layer at the interface between the solvent and the buffer solution. As a result, the absorption of the solvent by PDMS results in a self-formation of the lipid bilayer across the microchannel (Malmstadt et al. 2006). In this work we applied a new technology to confine the small amount of the lipid solution inside a microchannel by a push-pull junction capturing approach to make the array of the lipid bilayer inside a microchannel.

Figure 1 depicts the procedures for the push-pull junction capturing of the lipid solution. First, a buffer solution is pulled into the PDMS microchannel by applying a negative pressure at the outlet. The lipid solution is then pulled into the microchannel. By changing the direction of the syringe pump and creating the positive pressure at the microchannel's outlet, the

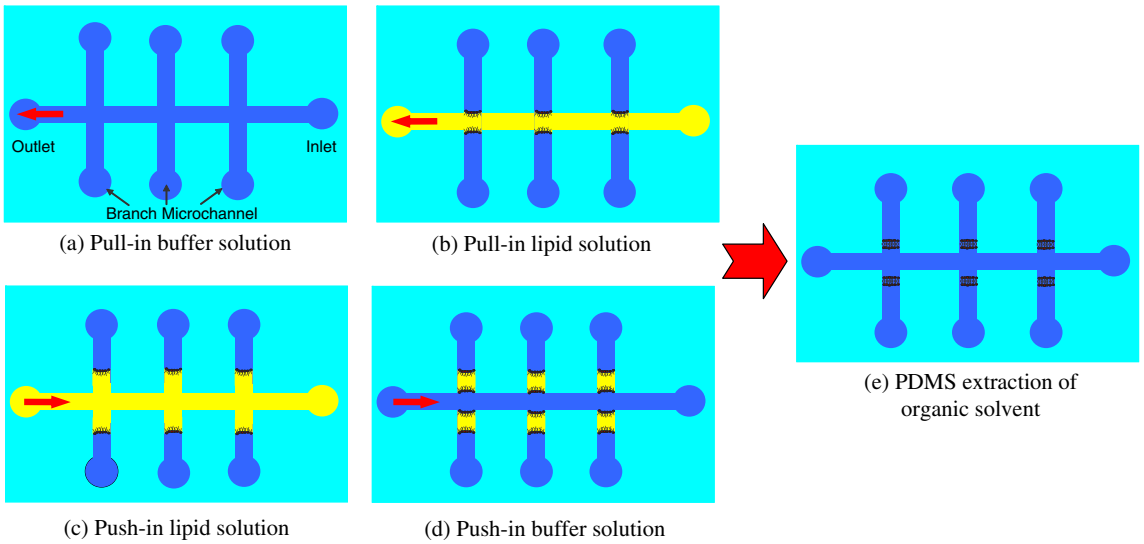

Fig. 1 Schematic illustration of push-pull junction capturing for a formation of multiple lipid bilayers inside an array of microchannel

solutions are pushed back into the microchannel. Because the pressure difference occurs at the junction of the microchannel during the change of flow direction, a small volume of organic solvent enters into each of the branch microchannels. As a result, when the buffer solution flows through the center microchannel, the organic solvent is captured at the entrance of the branch microchannels. As the hydrophilic head and the hydrophobic tail of the lipid come in contact with the buffer solution and the solvent respectively, the lipid bilayer membrane is generated across the branch microchannel after a complete absorption of solvent by the PDMS. After this self-formation of the lipid bilayer, the patterned electrode at the center microchannel and the branched microchannels allows high-throughput measurements of the lipid bilayers. To show the quality and feasibility of the lipid bilayer, the connector channel proteins of phi29 were inserted into the lipid bilayer, and current drops were successfully monitored during the insertion of the pore protein.

3 Material and methods

3.1 Design of microchannel

Figure 2 shows a schematic drawing of the designed microchannel. To achieve the array of lipid bilayer self-assembled across the microchannel, the microchannel has been designed to have one center microchannel and 20 branch microchannels. The center channel was designed to be 5 times wider than the branch microchannel. This design minimized the effect of flow variation at the center microchannel on the formed lipid bilayer. Also, small pressure drop at the center microchannel could be achieved due to a large cross-sectional area. Because the volume of captured solvent at the junction of branch microchannel depended on the pressure difference during push-pull driving of flow, the small pressure drop at the center microchannel accomplished the uniform amount of captured solvent at each branch microchannel.

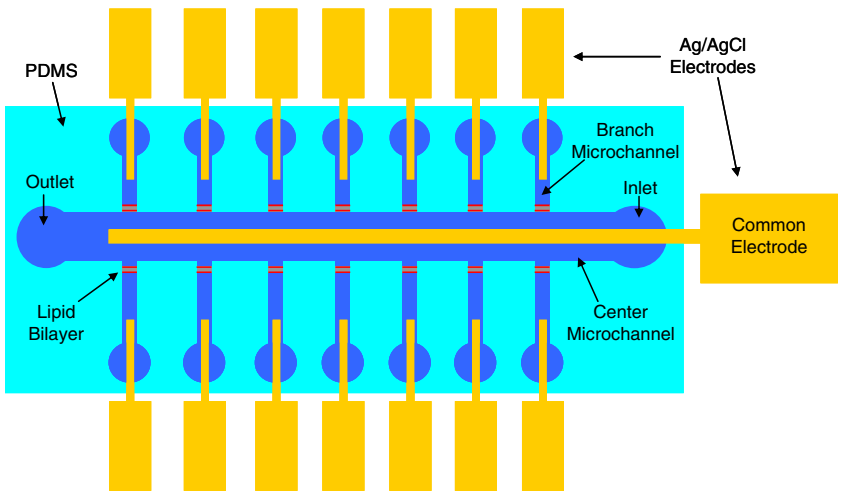

Fig. 2 Design of multiple lipid bilayers inside an array of microchannels

During the solvent absorption, the PDMS swelled up and the PDMS microchannel could be blocked. When the height of microchannel was less than 50 μm, the center microchannel was easily blocked and the lipid solvent could not flow through the microchannel. To avoid the blockage of microchannel by the deformation of PDMS, the microchannel was designed to be 100 μm high.

As the area of lipid bilayer was increased, the stability of lipid bilayer was degraded. Also, if the cross-sectional area of PDMS microchannel was too small, the microchannel could be blocked because of the PDMS swelling by the solvent absorption. After the experimental tests of various channel widths, the branch microchannels were designed to have a width of 100 μm with a square cross-section. With these considerations, the microchannel had a height of 100 μm, and a width of 500 μm for the center microchannel and 100 μm for the branch microchannel.

3.2 Preparation of lipid solution and lipid vesicle

The lipid solution was prepared in decane (Fisher Scientific Inc., USA) for the formation of lipid bilayer array inside the PDMS microchannel. For the preparation of the lipid solution, 20 % lipid in chloroform (Avanti Polar Lipids, Inc., USA) was dried by nitrogen gas-purging. The dried lipids were then re-dispersed in decane with 5 % concentration.

To prepare the nanopore-inserted lipid vesicles, 1 ml of 1 mg/ml phospholipid, 1,2-diphytanoyl-sn-glycerol-3-phosphocholine (DPhPC) was placed in a vial. The chloroform containing the lipids was evaporated by gentle nitrogen-purging in the hood, and the lipid vial was further dried overnight inside a vacuum chamber. On the second day, 2 ml of 200 mM sucrose was added to the vial with co-incubation with purified connectors (Wendell et al. 2009), which was then covered with Parafilm and stored overnight. An aliquot was taken from the middle of the solution and then transferred into a Petri dish. After settling, the vesicles were observed with epifluorescence microscopy.

3.3 Fabrication of the microfluidic channels

To fabricate the mold of the PDMS microchannel, standard soft-lithography process with SU-8 was performed on a Si substrate. The 3 in. Si wafer was dipped into the 2 % HF diluted in DI water to remove the SiO_2 layer on the Si substrate. Then, SU-8 2075 (Microchem Corp., USA) was spin-coated on the Si wafer with 1,500 rpm for 45 s to make a pattern thickness of 100 μm. Then, a prebaking of SU-8 was performed at 95°C for 30 min. After UV exposure for 50 s under a mask with the designed patterns, the exposed SU-8 was hard-baked at 95°C for 45 min. Then, the processed SU-8 was developed in SU-8 developer with a stirring of 100 rpm. The mixture of PDMS with a curing agent was casted on the mold, and placed on a leveled hot plate with the temperature of 50°C for 4 h.

The glass substrate was selected to assure a strong covalent bonding with the PDMS. Also, silver/silver chloride (Ag/AgCl) electrodes were patterned on the glass substrate for the electrochemical measurements. After rinsing and drying a microscope cover glass (Fisher Scientific Inc., USA), a metal deposition of titanium (Ti) and gold (Au) was performed with the thicknesses of 20 nm and 100 nm respectively. Using a lithography process with Shipley 1818 photoresist, the designed electrode was patterned on the cover glass by etching the Au/Ti layers. After the fabrication of Au/Ti electrodes, the Ag plating was performed with the current density of 0.1 mA/Cm^2 for 10 s, followed by Cl plating with the same current density for 5 s. Figure 3 shows the fabricated electrodes on the glass slide and the Ag/AgCl electroplated electrode.

After the fabrication of Ag/AgCl electrodes, the cured PDMS microchannel was bonded to the glass substrate by oxygen plasma treatment. The bonding side of the PDMS and the glass was treated for 15 s with a power of 75 W under 20 sccm of O_2 flowing. The plasma treated PDMS and glass was carefully aligned and bonded so that the Ag/AgCl electrodes were located at the center of microchannels. After the alignment of the microchannel and the electrodes, the bonded PDMS and glass slide was annealed at 80°C for 2 h.

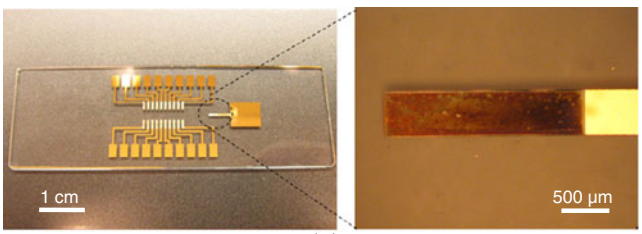

(a)

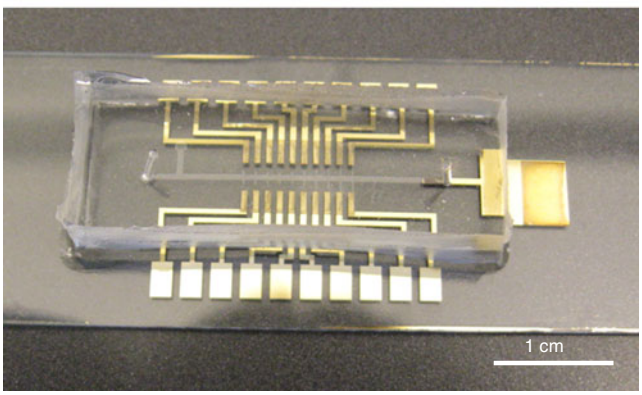

(b)

Fig. 3 Picture of the fabricated device. (**a**) patterned electrodes on glass substrate (*right*) and Ag/AgCl electrodes at the end of gold electrodes (*left*), and (**b**) attached PDMS microchannel

3.4 Electrical and optical monitoring for the insertion of phi29 connector

The electrodes at each microchannel were connected to a Axon Patch Clamp (Molecular Devices, LLC., USA) for the electrical characterization of the lipid bilayer. The electrode patterned at the center microchannel was shared as a common electrode, and the array of electrodes patterned at the branched microchannels were utilized to individually monitor the formed lipid bilayers at each branched microchannel. The current was measured between the center microchannel and the branch microchannels with an applied potential of 75 mV. The microscope and the syringe pump were installed inside the metal cage to reduce electrical noises. During the electrical measurement, the whole procedures to form the lipid bilayers were also observed by the microscope for simultaneous monitoring of the lipid bilayer, as can be seen in Fig. 4.

3.5 Microfluidic formation of lipid bilayer array

Because air bubbles in the microchannel blocked the ionic current flow through the phi29 nanopore embedded in the lipid bilayer, the fabricated microchannel should be filled with the buffer solution (1 M NaCl in DI water) without any captured bubbles inside the branch microchannel array. The branched microchannels did not have an outlet, and they were narrower than the center microchannel. Due to these geometrical restrictions, air was trapped at the branch microchannels, when the buffer solution flowed through the center microchannel. To avoid this generation of air bubbles, the PDMS microchannel was placed in a vacuum chamber for more than 1 h before the test. When the PDMS microchannel was placed inside the vacuum chamber, the air was released from the PDMS. The squeezed PDMS then absorbed air bubbles inside the microchannels under an atmospheric pressure (Monahan et al. 2001). With this method, the captured air bubbles at the branched microchannel could be completely removed.

The prepared bubble-free microchannel was stayed for 12 h to saturate the PDMS channel with the buffer solution. Because water and solvent were immiscible, the rate of solvent absorption by the PDMS microchannel was decreased. When the solvent was absorbed too quickly, the lipid bilayer was easily broken during the formation process. Thus, by saturating the PDMS microchannel with the buffer solution, a stable formation of lipid bilayers could be attained with high yield of success at each microchannel.

After connecting the inlet tube to the microchannel, a negative pressure was applied at the outlet of the microchannel. The buffer solution and the lipid solvent were sequentially pulled into the microchannel at a flow rate of 10 μl/min. As soon as the lipid solvents filled the microchannel, the flow direction was reversed by applying positive pressure at the outlet. While the lipid solvent was pushed into the center microchannel, the pressure difference was created at the branched microchannel, which led the intrusion of the lipid solvent into the branched microchannels. Once the buffer solution flowed through the center channel, the intruded lipid solvent was captured between the buffer solutions. After the lipid solvent was captured, the flow of the buffer solution was stopped to prevent a pressure change during the lipid bilayer formation. Finally, the absorption of the captured solvent by PDMS attained the formation of the lipid bilayer across the microchannel.

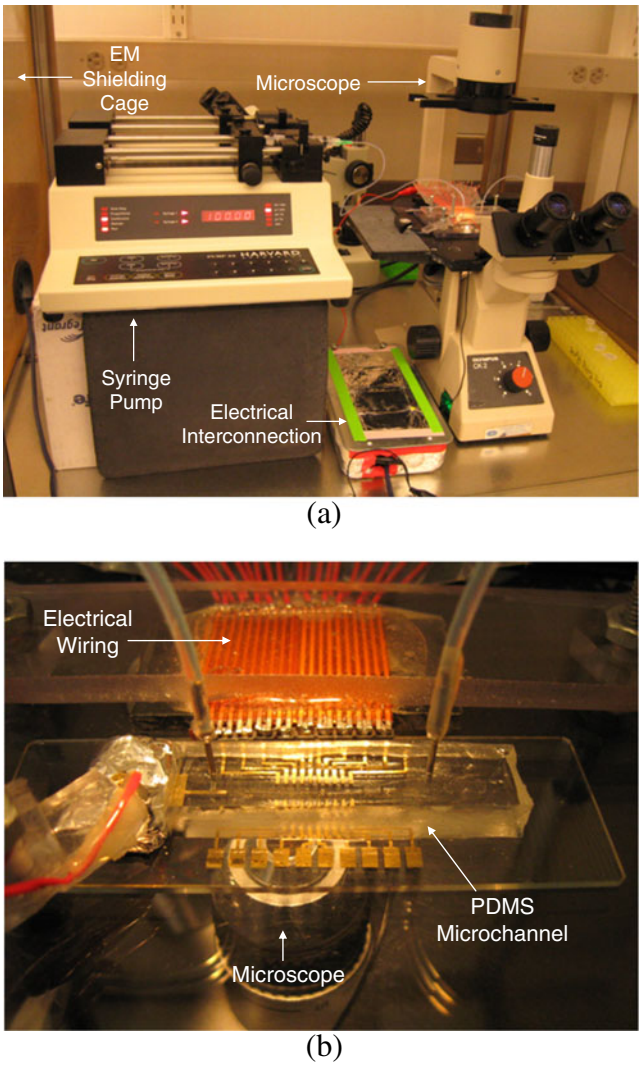

Fig. 4 Picture of the microfluodics showing the experimental set-up. (**a**) The systme inside EM shielding cage. (**b**) Electrical connection to each electrode on the microscope for visualizing the formation of lipid bilayer with electrical monitoring

4 Results and discussion

Figure 5(a) shows the array of junction-captured lipid solutions inside the microchannels. The captured solutions were

extracted by the PDMS as sequentially pictured in Figure 5(b), leaving the lipids to form the bilayer membrane. This method efficiently formed the lipid bilayer array with a high level of success. To clearly demonstrate the yield of successful lipid bilayer formation, a video file has been provided in Supporting information. In the video file, after all the procedures of lipid bilayer formation, the examination of each microchannel was carried out to check the successful formation of lipid membrane. As shown in the video file, each of the 20 branched microchannels has a lipid bilayer at the entrance of the microchannels. Utilizing the described conditions of flow rate, lipid solution concentration, and preparation steps of PDMS microchannel, a high yield of lipid bilayer formation was reproducibly achieved.

Figure 5(c) shows a microscopic picture of an enlarged example of the lipid bilayers. The picture shows a thin line of lipid membrane across the microchannel. Considering the thickness of the lipid bilayer (5~6 nm), the microscopic picture of the lipid bilayer seems to have multiple layers of lipids. However, because the structure of the lipid bilayer usually has a gibbs-plateau border at the interface between the lipid bilayer and the microchannel wall, the thickness at the center part of the lipid bilayer would be on the nano scale, which cannot be seen in the microscopic image (White et al. 1986).

To prove the thickness of lipid bilayer, the lipid bilayer was analyzed by electrically measuring the bilayer's capacitance. The measured capacitance was found to be 45 pF, and the thickness of the bilayer (d) could be calculated utilizing the following equation,

$$d = \frac{\varepsilon_0 \varepsilon_s A}{C} \quad (1)$$

where ε_0 and ε_s are the permittivity of free space (8.854×10^{-12} F•m^{-1}) and lipid (~3; no units, relative) respectively, while A is the cross-sectional area of the branched microchannel (Dilger et al. 1979). The calculated thickness of the lipid bilayer was 6.2 nm. Considering the length of a single lipid (2.5 nm), the thickness was slightly larger than the length of two lipids. Because annulus lipids accumulated at the interface between the walls of the microchannel and the lipid bilayer, the average thickness of the lipid bilayer would be thicker than the bilayer thickness of lipids.

Additionally, an electrical measurement for the insertion of a pore protein was performed. Without the insertion of a pore protein, the current path is blocked by the lipid bilayer, resulting in zero current through the membrane. However, once the pore protein is inserted into the lipid bilayer, the current is able to flow through the inserted pore. So, a current level sharply changes during and after the insertion of the pore protein at the lipid bilayer.

For high throughput analysis of the nanopore inserted lipid bilayer, current traces from 10 lipid bilayers were recorded as

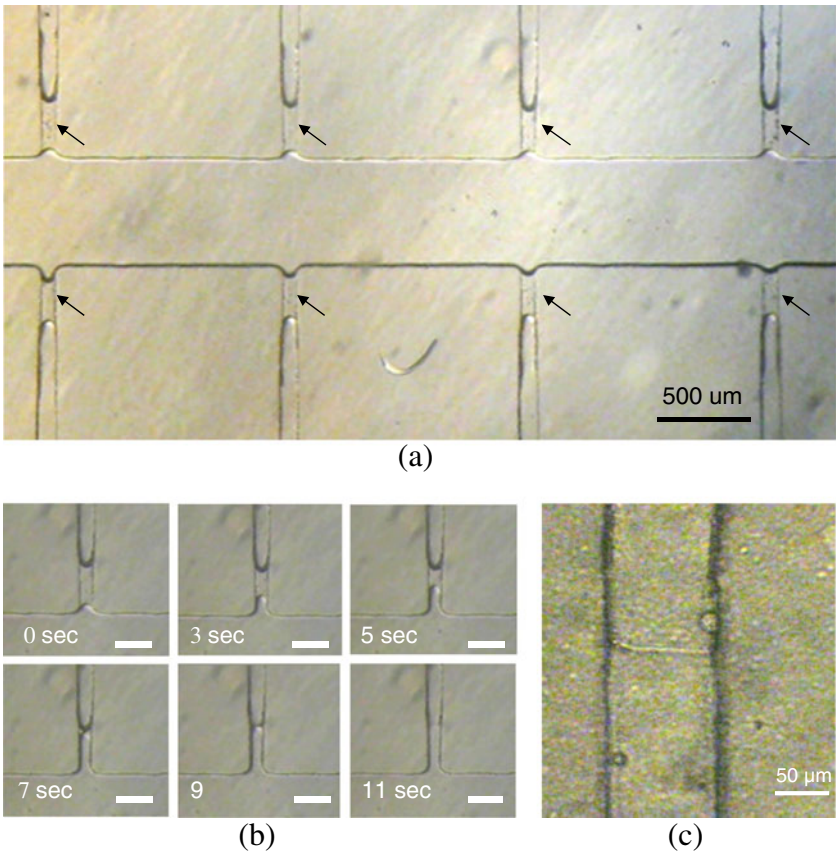

Fig. 5 Microscopic pictures for the formation of lipid bilayer array. (**a**) Array of the captured lipid solutions at the entrance of branch microchannels, (**b**) sequential pictures of lipid bilayer formation by solvent absorption through PDMS (200 μm scale bar), and (**c**) enlarged microscope picture of lipid bilayer

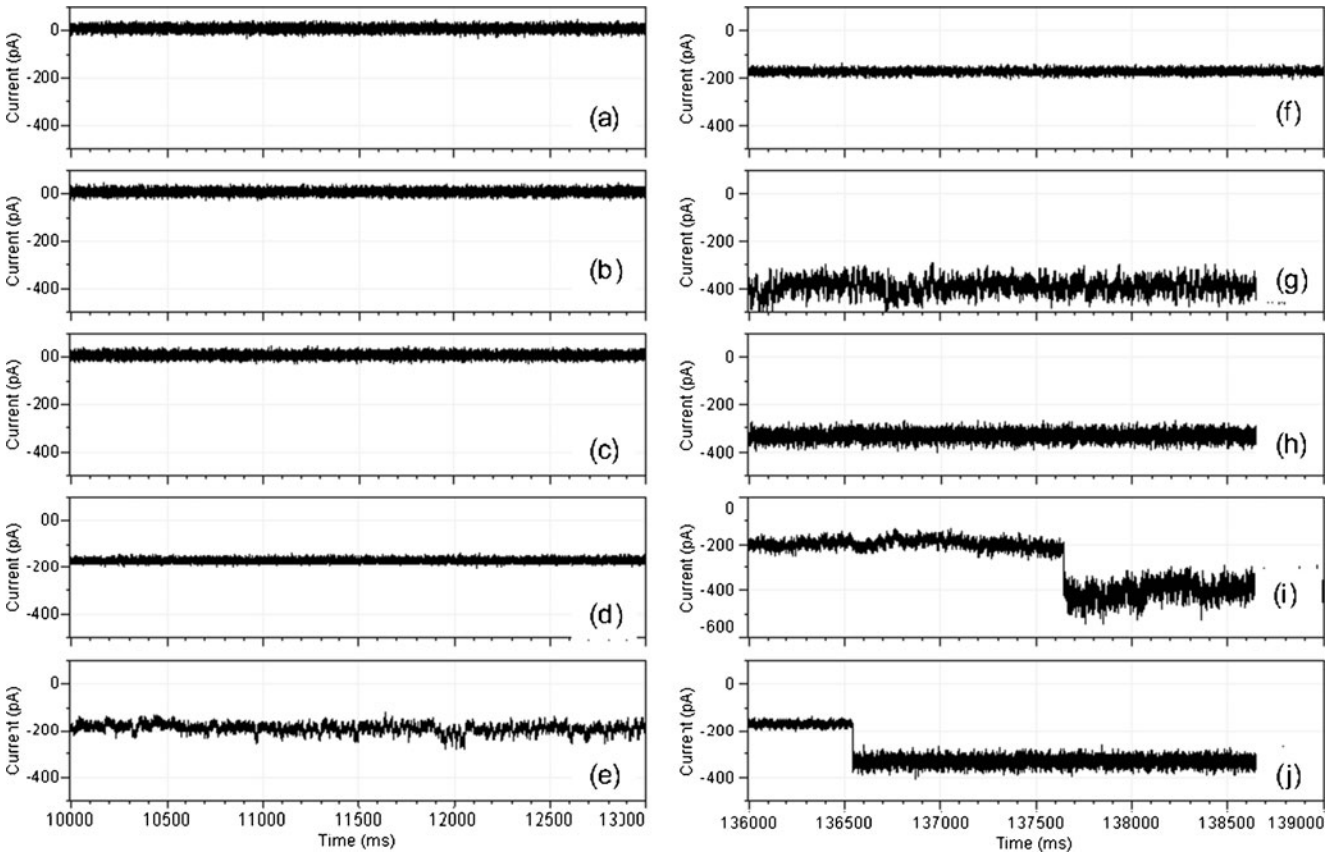

Fig. 6 Current traces from 10 lipid bilayers with different numbers of the inserted phi 29 nanopore. (**a**~**c**) 0 inserted nanopore, (**d**~**f**) 1 inserted nanopore, (**g**~**h**) 2 inserted nanopores, and (**i** and **j**) current trace during the phi 29 nanopore insertion

shown in Fig. 6. Since each lipid bilayer contained different numbers of the inserted phi 29 nanopore, different current levels were measured according to the insertion numbers of the phi 29 nanopore. When the concentration of buffer solution was 1 M NaCl with the applied potential of 75 mV, the current was dropped averagely 200 pA for each insertion of the phi 29 nanopore, which was equal to 2.7 n Siemens of conductivity. The resulted current drop clearly indicated the insertion of the pore protein at the lipid bilayer membrane in the fabricated channel array. Also, this insertion of a pore protein verified that the lipid membrane has a bilayer quality. If the lipid membrane has multiple layers of lipids, thick lipids

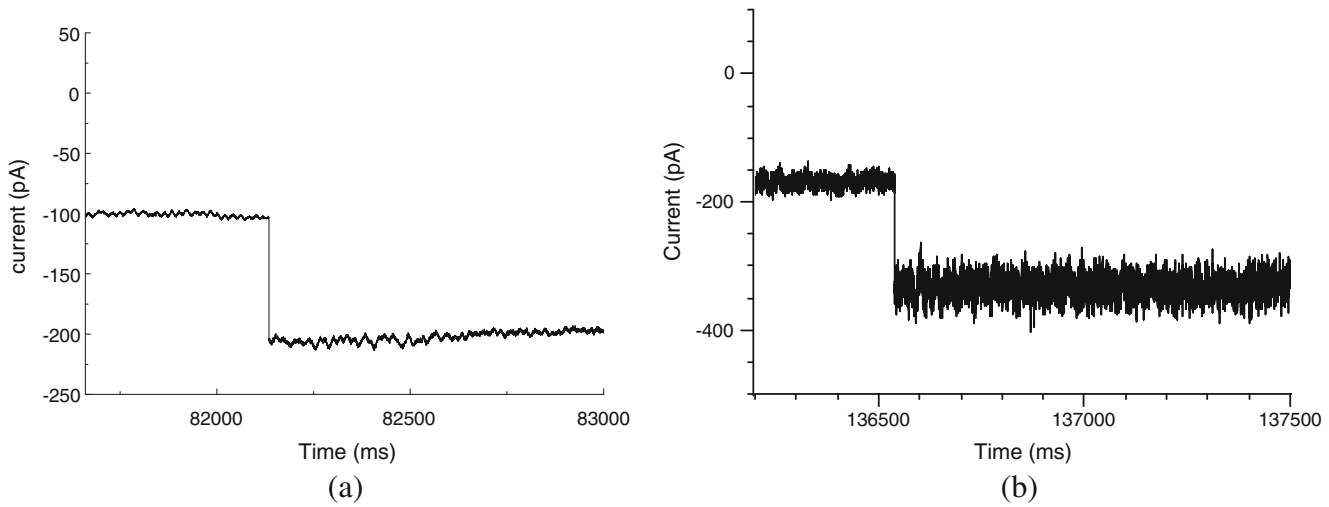

Fig. 7 Current trace of phi29 connector protein molecule inserted into a microfluidic lipid-bilayer in (**a**) 500 mM NaCl buffer solution and (**b**) 1 M NaCl buffer solution

membrane would prevent the pore protein from making a current path through the multiple layers of lipids. Therefore, the result of a current drop further proved the bilayer constitution of the lipids, showing a similar structure with a membrane of mammalian cells.

For further characterization on the phi29 nanopore membrane, two concentrations of the NaCl solution was tested, where one was 0.5 M and the other was 1 M as depicted in Fig. 7(a) and (b). Since the noise was generated by the ionic interaction with the fabricated Ag/AgCl electrodes, the signal for 1 M NaCl contained higher noise level than the one for 0.5 M NaCl. When the concentration was 0.5 M NaCl with the potential of 75 mV, the current drop by the connector channel was 112 pA which is, equal to 1.5 n Siemens. In case of 1 M NaCl and 75 mV, the current drop was 200 pA, equal to 2.7 n Siemens of conductivity. The two parameters are closely matched to our previous measurement (1.56±0.16 nS for 0.5 M NaCl and 3.21±0.51 nS for 1 M NaCl) by classical single channel recording setup under the same ion strengths (Wendell et al. 2009). These coincidences demonstrated a feasibility in using the microfluidic system for monitoring the connector channel for further development of single pore sensing and high throughput single pore dsDNA sequencing using the phi29 motor channel nanopore.

5 Conclusions

In this work, an array of a PDMS microchannel was applied to form an array of lipid bilayers for high-throughput screening of nanopore biosensing. With the microfluidic technique of push-pull junction capturing, a small amount of lipid solution could be easily captured at the junctions of a microchannel array. After solvent extraction by PDMS, an array of lipid bilayer membrane was formed at the entrance of each microchannel with a high yield of success. To show a functionality of the formed lipid bilayer, the phi29 nanopore connector protein was successfully inserted into the lipid bilayer under the electrical and optical monitoring. The result shows a stable and reproducible formation of the lipid bilayer array with a high quality of bilayer thickness, which is highly desirable for monitoring the interaction of the lipid bilayer with biological components. As a result, the developed technique can be applied to various researches with the lipid bilayer membrane on a lab-on-a-chip platform.

Acknowledgments Supported by NIH grants EB012135 (P. G.) as well as NIH Nanomedicine Development Center: Phi29 DNA Packaging Motor for Nanomedicine, through the NIH Roadmap for Medical Research (PN2 EY 018230) (P.G.). P.G. is a co-founder of Kylin Therapeutics, Inc, and Biomotor and Nucleic Acid Nanotechnology Development Corp, Ltd.

References

A. Manz, H. Becker, *Microsystem Technology in Chemistry and Life Science* (Springer, 1998).
B. Le Pioufle, H. Suzuki, K.V. Tabata, H. Noji, S. Takeuchi, Anal. Chem. **80**, 328 (2008)
C.H. Ahn, C. Jin-Woo, G. Beaucage, J. Nevin, L. Jeong-Bong, A. Puntambekar, J.Y. Lee, Proc. IEEE **92**, 154 (2004)
C. Ibanez, J. A. Garcia, J. L. Carrascosa, M. Salas, Nucleic Acids Res. **12**, 2351 (1984)
D. Shu, H. Zhang, J. Jin, and P. Guo, EMBO J. **26**, 527 (2007)
D. Wendell, P. Jing, J. Geng, V. Subramaniam, T.J. Lee, C. Montemagno, P. Guo, Nat. Nano. **4**, 765 (2009)
F. Haque, J. Lunn, H. Fang, D. Smithrud, P. Guo, ACS Nano. **6**(4), 3251–3261 (2012)
F. Xiao, J. Sun, O. Coban, P. Schoen, J. C. Wang,. R. H. Cheng, P. Guo, ACS Nano **3**, 100 (2009)
F. Zhang, S. Lemieux, X. Wu, S. St. Arnaud, C.T. McMurray, F. Major, and D. Anderson, Mol. Cell. **2**, 141 (1998)
H. Fang, P. Jing, F. Haque, P. Guo, Biophysical Journal **102**, 127 (2012)
H. Suzuki, S. Takeuchi, Anal. Bioanal. Chem. **391**, 2695 (2008)
H. Suzuki, K.V. Tabata, H. Noji, S. Takeuchi, Biosens. Bioelec. **22**, 1111 (2007)
H. Suzuki, K.V. Tabata, H. Noji, S. Takeuchi, Langmuir **22**, 1937 (2006)
J. Geng, H. Fang, F. Haque, L. Zhang, P. Guo, Biomaterials **32**, 8234 (2011)
J.C. McDonald, G.M. Whitesides, Acc. Chem. Res. **35**, 491 (2002)
J.L. Poulos, T. Jeon, R. Damoiseaux, E.J. Gillespie, K.A. Bradley, J.J. Schmidt, Biosens. and Bioelec. **24**, 1806 (2009)
J. Monahan, A.A. Gewirth, R. Nuzzo, Anal. Chem. **73**, 3193 (2001)
J.P. Dilger, S.G. McLaughlin, T.J. McIntosh, S.A. Simon, Science **206**, 1196 (1979)
K. Aathavan, A.T. Politzer, A. Kaplan, J.R. Moffitt, Y.R. Chemla, S. Grimes, P.J. Jardine, D.L. Anderson, and C. Bustamante, Nature **461**, 669 (2009)
K. Funakoshi, H. Suzuki, S. Takeuchi, Anal. Chem. **78**, 8169 (2006)
M. A. Robinson et al., Nucleic Acids Res. **34**, 2698 (2006)
M.E. Sandison, M. Zagnoni, H. Morgan, Langmuir **23**, 8277 (2007)
N. Malmstadt, M.A. Nash, R.F. Purnell, J.J. Schmidt, Nano. Lett. **6**(9), 1961 (2006)
P. Guo, S. Erickson, and D. Anderson, Science **236**, 690 (1987a)
P. Guo, C. Peterson, and D Anderson, J. Mol. Biol. **197**, 219 (1987b)
P. Guo, C. Zhang, C. Chen, M. Trottier, and K. Garver, Mol. Cell. **2**,149 (1998)
P. Guo, Prog. Nucleic Acid Res. Mol. Biol. **72**, 415 (2002)
P. Jing, F. Haque, A. Vonderheide, C. Montemagno, P. Guo, Mol. BioSys. **6**, 1844 (2010a)
P. Jing, F. Haque, D. Shu, C. Montemagno, P. Guo, Nano Lett. **10**(9), 3620 (2010b)
P. Yager, T. Edwards, E. Fu, K. Helton, K. Nelson, M.R. Tam, B.H. Weigl, Nature **442**, 412 (2006)
R.E. Oosterbroek, A. van den Berg, *Lab-on-a-Chip; Miniaturized Systems for (BIO)Chemical Analysis and Synthesis* (Elsevier B.V, Amsterdam, 2003)
S. H. White, The physical nature of planar bilayer membranes in Ion Channel Reconstitution, C. Miller, Ed. Plenum Press, NY. pp. 3-35. (1986)
S. Ota, H. Suzuki, S. Takeuchi, Lab. Chip. **11**, 2485 (2011)
T. Osaki, H. Suzuki, B. Le Pioufle, S. Takeuchi, Anal. Chem. **81**, 9866 (2009)
Y. Cai, F. Xiao, P. Guo, Nanomedicine 4, 8 (2008)
Y. Guo, F. Blocker, F. Xiao, P. Guo, J. Nanosci. Nanotechnol. **5**, 856 (2005)